NIH Public Access
Author Manuscript
Shock. Author manuscript; available in PMC 2013 March 1.

Published in final edited form as:
Shock. 2012 March ; 37(3): 297–305. doi:10.1097/SHK.0b013e318240b59b.

Disruption of the Mucosal Barrier during Gut Ischemia Allows Entry of Digestive Enzymes into the Intestinal Wall

Marisol Chang, **Erik B. Kistler**, and **Geert W. Schmid-Schönbein**
Department of Bioengineering, Institute of Engineering in Medicine, University of California San Diego, La Jolla, CA 92093–0412

Abstract

Intestinal ischemia is associated with high morbidity and mortality but the underlying mechanisms are uncertain. We hypothesize that during ischemia the intestinal mucosal barrier becomes disrupted, allowing digestive enzymes access into the intestinal wall initiating autodigestion. We used a rat model of splanchnic ischemia by occlusion of the superior mesenteric and celiac arteries up to 30 min with and without luminal injection of tranexamic acid as a trypsin inhibitor. We determined the location and activity of digestive proteases on intestinal sections with in-situ zymography and we examined the disruption of two components of the mucosal barrier: mucin isoforms and the extra- and intracellular domains of E-cadherin with immunohistochemistry and western blot techniques. The results indicate that non-ischemic intestine has low levels of protease activity in its wall. After 15 min ischemia protease activity was visible at the tip of the villi and after 30 min enhanced activity was seen across the full thickness of the intestinal wall. This activity was accompanied by disruption of the mucin layer and loss of both intra- and extracellular domains of E-cadherin. Digestive protease inhibition in the intestinal lumen with tranexamic acid reduced morphological damage and entry of digestive enzymes into the intestinal wall. This study demonstrates that disruption of the mucosal epithelial barrier within minutes of intestinal ischemia allows entry of fully activated pancreatic digestive proteases across the intestinal barrier triggering autodigestion.

Keywords

Shock; mucin; serine proteases; e-cadherin

INTRODUCTION

Ischemic injury of the small intestine due to reduced perfusion of the splanchnic circulation can result from different conditions, e.g. small bowel obstruction (1), arterial and venous thrombosis (2), and ischemia after cardiac and other surgical procedures (3). Splanchnic ischemic injury increases the risk of developing shock and multiple organ failure (4–7) with consequent high morbidity and mortality (8–10). Increasing evidence suggests that pancreatic digestive enzymes play an important role in different models of shock (11–14). Blockade of digestive enzymes in the lumen of the intestine prior to ischemia prevents intestinal cell dysfunction, generation of inflammatory and/or cytotoxic mediators and their leakage into the systemic circulation (15–17).

Correspondence: Dr. Geert W. Schmid-Schönbein, Microcirculation Laboratory, Department of Bioengineering, Institute of Engineering in Medicine, University of California San Diego, 9500 Gilman Drive, La Jolla, CA 92093-0412 USA, (858)534-3852, (858)534-5722, (fax) gwss@ucsd.edu.

NIH-PA Author Manuscript
NIH-PA Author Manuscript
NIH-PA Author Manuscript

NIH-PA Author Manuscript

NIH-PA Author Manuscript

NIH-PA Author Manuscript

Under normal physiological conditions, pancreatic proteases are compartmentalized in the intestinal lumen by the mucosal barrier. This barrier can be divided into two major components, the mucus layer and the epithelium. Mucin glycoprotein is the major constituent of the mucus barrier (18) whereas enterocytes with their adherens and tight junctions make up the epithelial barrier (19). During ischemia the integrity of the mucosal and epithelial barriers become compromised (20, 21); our hypothesis is that disruption of these barriers during intestinal ischemia allows pancreatic digestive enzymes to enter the intestinal wall and thereby exacerbate intestinal injury.

In this study we examined the levels of enzymatic activity in the intestinal wall and the degree of mucosal barrier disruption in a pre-injury model (early periods of intestinal ischemia) since longer ischemia and reperfusion result in severe intestinal injury. For this purpose we studied two mucin isoforms: mucin2, the main component of goblet cell-derived mucin found in the mucus layer lining the small intestine and mucin13, a membrane-bound mucin; we also studied intra- and extracellular domains of e-cadherin, the main interepithelial adhesion molecules. In addition, we determined the extent to which enteral injection of tranexamic acid, a trypsin and plasminogen inhibitor (22, 23), prior to ischemia inhibited enzymatic activity in the intestinal wall. Furthermore, we determined whether digestive enzymes achieve systemic access after entering the intestinal wall and whether this is prevented by enteral tranexamic acid treatment.

MATERIALS AND METHODS

Animal Groups

All animal protocols were reviewed and approved by the University of California San Diego Animal Subjects Committee. Male Wistar rats (300–350g, Harlan Sprague Dawley Inc, Indianapolis, IN) were randomly assigned to one of five groups: a sham group (SHAM), two ischemic groups with splanchnic arterial occlusion (SAO) for 15 and 30 min (SAO15, SAO30) and two ischemic SAO groups with enteral tranexamic acid (TA) treatment (SAO15+TA, SAO30+TA); n=4 per group.

SAO Model

Rats were kept on solid food restriction with water ad libitum for 12 hours prior to surgery, tranquilized with Xylazine (20 mg/ml, 0.2 μL/g BW) and anesthetized with Nembutal (50 mg/ml, 1 μL/g BW), followed by cannulation of the left femoral vein and artery. In the SHAM and SAO groups 0.9% normal saline (NS) without pH adjustment, 3ml/100g BW, was injected into the lumen of the intestine while in the treatment group (SAO+TA) tranexamic acid (Sigma Scientific, St. Louis, MO), ~200 mM (0.3 g for a 300g rat), in NS was used. After 30 min the superior mesenteric and celiac arteries were isolated and ligated (SAO and SAO+TA groups) or isolated without ligation (SHAM). Animals were euthanized after 30 min (SHAM) and after 15 or 30 min (SAO and SAO+TA).

Tissue Processing

Jejunal segments (~1 cm in length) were excised without removal of luminal contents, suspended in Tissue-Tek O.C.T. Compound (Sakura Finetek, Torrance, CA), snap frozen in isopentane/liquid nitrogen, and stored in −80°C for further analysis. Cryosections (5 μm thickness) along the longitudinal axis of the villi were used throughout all experiments.

Intestine homogenates: in separate experiments, 1cm equally spaced segments of the intestine were excised. For Western blot assays luminal contents were washed with NS; followed by homogenization with CelLytic™(Sigma) in the presence of protease inhibitors (5mM EDTA, 5mM N-Ethylmaleimide, 25mM iodoacetamide, 5mM benzamidine, 300mM

NIH-PA Author Manuscript

NIH-PA Author Manuscript

NIH-PA Author Manuscript

acarbose, 5mM 6-aminocaproic acid, 1mM protease inhibitor cocktail, (Sigma Scientific)) to inhibit further degradation. For enzyme activity assays intestinal luminal contents were retained to measure enzyme activity in the whole intestine; homogenization with CelLytic™ was done without addition of protease inhibitors. Homogenates were centrifuged (16,000g for 15 min at 4°C), the supernatant was collected and protein concentration was assessed with the bicinchoninic acid protein assay (Thermo Scientific, Rockford, IL).

Luminal contents

In separate experiments the small intestine of sham animals were excised, the luminal contents were flushed with 20 ml NS and luminal contents were centrifuged (16,000g for 15 min at 4°C); the supernatant was collected and protein concentration was determined.

Western Blot

Experiments were performed in a standard fashion (24); 20μg of protein were used for each sample of intestine homogenate. Primary antibodies were diluted as followed: mucin2 and mucin13 1:1000 (Santa Cruz Biotechnology, Santa Cruz, CA), trypsin 1:1000 (Santa Cruz Biotechnology), chymotrypsin 1:300 (Abcam, Cambridge, MA), elastase 1:1000 (Lifespan Biosciences, Seattle, WA), and for the intra- and extra-cellular domains of E-cadherin 1:300 (Abcam). Secondary antibodies were diluted at 1:20000 (Santa Cruz Biotechnology) and detected with Super Signal West Pico (Thermo Scientific). The exposed x-ray films were scanned and analyzed using the gel analysis tool of the NIH ImageJ software.

Enzyme Activity

All chemicals were purchased from Sigma Scientific. The activity of intestine homogenates (100μg of protein), luminal contents (50μg of protein), or 50μg/ml purified enzyme (porcine trypsin and elastase, and bovine chymotrypsin) was measured with 50mM substrates specific for chymotrypsin (glutaryl-L-phenylalanine 7-amido-4- methylcoumarin), trypsin and papain (Nα-benzoyl-L-arginine-7-amido-methylcoumarin hydrochloride), and leukocyte and pancreatic elastase (N-methoxysuccinyl-Ala-Ala-Pro-val-7-amido-4-methylcoumarin) as previously described (25–27). The initial rates of hydrolysis were measured by the fluorescent intensity of 7-amido-4-methylcoumarin (SpectraMax Gemini XS, Molecular Devices) at 380/460 nm (excitation/emission). The enzymatic inhibitory properties of TA (300mM, 160mM and 50mM) were determined by incubation of the purified enzymes with TA for 1 hour, followed by incubation with specific substrates as above. The initial velocity of the reaction was calculated as the rate of fluorescent units per μg of protein per minute. The data was fitted with a non-linear regression of Michaelis-Menten equation and V_{max} K_m, Ki, were computed with GraphPad Prism (Graphpad Software. San Diego, CA).

In-situ Zymography

Digestive enzyme activity was assessed by fluorescence intensity measurements resulting from proteolytic cleavage of substrates (28, 29) specific for chymotrypsin (2mM), trypsin (1mM) and elastase (1mM), as above. Each substrate was diluted to its final concentration in 1% low melting point agarose (Sigma Scientific) and maintained at 37°C. 10μl substrate was added on sections thawed at 37°C followed by gelation for 5 min at 4°C. The tissue/ substrate was incubated for 1 hour at 37°C and immediately observed with an inverted microscope (20X objective).

Histology, immunohistochemistry and alcian blue staining

Cryosections were fixed for 10 min in cold acetone and stained with standard hematoxylin/ eosin or immunohistochemistry techniques. Primary antibodies were diluted as followed: mucin2 and mucin13 1:200 (Santa Cruz Biotechnology); intracellular domain of E-cadherin

NIH-PA Author Manuscript

NIH-PA Author Manuscript

NIH-PA Author Manuscript

1:300 (Abcam); extracellular domain of E-cadherin 1:250 (Abcam) and secondary antibodies (ImmPRESS, Vector Lab) The slides were developed using 3,3′-diaminodbenzidine substrate and counterstained with hematoxylin (Vector Lab). Alcian blue was used to label the carbohydrate mucin moiety. Briefly, cryosections were fixed in Carnoy's fixative for 10 min, stained in 1% alcian blue solution in 3% acetic acid, (pH 2.5) for 30 min, and counterstained with hemotoxylin. Slide sections were observed in a non-blinded fashion under an inverted microscope (20X and 60X objectives).

In-situ zymography/immunohistochemistry

The simultaneous visualization of enzyme activity and mucin was carried out using a modified protocol (30). Cryosections were fixed in 95% cold ethanol and protease activity was detected via proteolytic cleavage of fluorescent BODIPY TR-X casein 10 μg/ml (EnzChek®, Invitrogen, Carlsbad, CA) on tissue sections after 1-hour incubation at 37°C. Subsequently, sections were fixed with 4% paraformaldehyde for 15 min, incubated overnight with mucin2 1:200 primary antibody and FITC secondary antibody 1:10000 (Santa Cruz Biotechnology) and observed on an inverted microscope (20X objective) using the appropriate fluorescent filters.

Gelatin zymography

Heparinized blood from the femoral artery was collected one minute before euthanasia, centrifuged (2,000 g for 15 min), aliquoted, and stored at − 80°C until use. Plasma samples (0.6 μl), with a single freeze/thaw cycle were loaded into 12% SDS acrylamide gels cross-linked with gelatin (1 mg/ml); all buffers and protocols were performed as previously described by Hibbs (31).

Image Analysis

Images were processed with NIH ImageJ software, followed by measurements of the fluorescent or light intensities in digital units (D.U). Mean fluorescent or light intensity is defined as the sum of all pixel intensities divided by the sum of all pixels in the selected area (D.U./pixel). Enzymatic activity in the intestinal tissue was measured as the mean fluorescent intensity on micrographs of four cryosections per animal (n=4) per group. A rectangular area covering 2–3 villi from the villi tips to the muscle was selected for each micrograph; the intestine was outlined and the mean fluorescent intensity was calculated on the outlined area. The enzyme penetration from the tip to the intestinal wall was determined as the mean fluorescent intensity on an area covering a single villus; each intestinal cross-section was further divided into five regions from the villus tip to the serosa: villus tip, mid villus, crypt and muscularis mucosa, submucosa, and muscularis externa. Sixteen villi were measured over four sections per animal (n=4) per group. Mucin2 density was measured as the mean light intensity in a rectangular area covering 2–3 villi was selected for all groups. Images were thresholded so only mucin staining was visible; five tissue sections per animal (n=4) per group were analyzed. Mucin13 density was determined by placing a one-pixel wide line perpendicular to the epithelium; a profile plot of the light intensity values along the line was generated for 25 lines measured over four intestinal sections per animal (n=4). The plot profiles were aligned with respect to the maximum light intensity and then averaged. The average of these maximum intensity values were selected as measure for mucin13 density. Mucin2 and protease activity co-localization was determined on simultaneously captured protease activity (red channel) and mucin density (green channel) micrographs. An area covering one villus was consistently selected for each group; each area was further divided into four regions: villus tip, mid villus, crypt, submucosal, and muscle layer. The mean fluorescent intensity over each region was measured for each channel. Twenty villi over four tissue sections per animal (n=4) per group were selected. E-cadherin density was determined as the mean light intensity on a rectangular area covering

NIH-PA Author Manuscript

NIH-PA Author Manuscript

NIH-PA Author Manuscript

the villus tip. The selected area was determined by setting a threshold so only E-cadherin staining was visible; twenty villi over four tissue sections per animal (n=4) per group were analyzed.

Statistical Analysis

Results are presented as mean±SEM. Unpaired comparisons of mean values between groups were carried out by one-way ANOVA followed by Bonferroni post-hoc. $P<0.05$ was considered significant.

RESULTS

In-vitro and in-vivo inhibition of digestive enzymes by tranexamic acid (TA)

we determined in-vitro the ability of TA to inhibit digestive enzymes [50μg/ml] (Figure 1A); enzyme kinetic parameters are shown in (Figure 1B). Our data shows that TA inhibited trypsin in a competitive manner with an inhibition constant of 56.5mM; however TA did not effectively inhibit chymotrypsin or elastase. The activity and protein levels of these digestive enzymes in the luminal contents (50μg of protein) of SHAM animals are shown in (Figure 2A–C); we found high activity of these enzymes with trypsin having the highest activity. We also tested the ability of TA (~200mM) to inhibit these digestive enzymes in-vivo (Figure 2D); both trypsin and chymotrypsin activity in whole intestine homogenates significantly increased after 30 min of ischemia compared to sham animals. Whole intestinal homogenates in the TA treatment groups displayed a trend that shows a decreased trypsin and chymotrypsin activity; elastase activity did not differ among groups. Protein levels of these enzymes remained constant among all groups for all three enzymes (Figure 2E, F).

Intestinal morphology

Normal villi with intact epithelial cells were observed in the sham experimental group (Figure 3A, B). After 15 minutes ischemia lesions developed in the subepithelial spaces and epithelial cells were denuded near the tips of the villi. After 30 min ischemia pronounced injury was seen with complete degradation of the villus tip, a further decrease in villi length and increase in villi thickness; which is indicative of edema. Enteral treatment with TA prevented villus injury but did not prevent reduction in villi length or increase villi thickness (Figure 3B).

Enzyme activity in the intestinal wall

Next we determined whether digestive enzymes are able to enter the wall of the intestine during intestinal ischemia. Activity of trypsin, chymotrypsin and elastase were minimal in the mucosa of the sham group but significantly elevated in the ischemic groups and decreased to almost baseline in the enteral TA treatment groups (Figure 4A, B). At 15 min ischemia the three different enzymes were observed to penetrate the epithelium at the villus tips. By 30 min ischemia, the villi displayed significant enzymatic activity from the villi tips to the crypts and serosa (Figure 4C). We confirmed these results with Western blot analysis of intestine homogenates which demonstrated significantly increased protein levels of trypsin and chymotrypsin in the wall of the intestine after 30 min ischemia and decreased levels after TA treatment as compared to sham controls (Figure 4D, E).

Mucin isoforms in the rat intestine

To determine to what degree the mucin component of the mucosal barrier is disrupted during ischemia we labeled the mucin density by several methods (Figure 5A). Mucin carbohydrate density decreased in the villi of the ischemic groups and to a lesser extent in the TA treatment groups (Figure 5B). In the lumen however, ischemia significantly

NIH-PA Author Manuscript

NIH-PA Author Manuscript

NIH-PA Author Manuscript

decreased mucin carbohydrate density, which was reversed by treatment with TA (Figure 5B). The preservation of mucin carbohydrates in the presence of TA suggests that mucin carbohydrate disruption is mediated at least in part by a proteolytic mechanism (Figure 5A, B). Mucin2 in goblet cells (Figure 5A) did not change among groups but was decreased in the intestinal lumen of both ischemic and TA treatment groups (Figure 5B). Total mucin2 density (villi+lumen) decreased in ischemia with and without TA, suggesting that mucin2 is disrupted by ischemia, but less likely via a proteolysis (Figure 5C). Conversely, the density of membrane bound mucin (mucin13) (Figure 5A) was decreased in the ischemic groups but was restored by TA treatment (Figure 5B). Western blot analysis of mucin2 and mucin13 confirmed decreased protein levels of both mucin2 and mucin13 during ischemia. Protein levels were similar to sham control in the TA treatment group for mucin13 but not mucin2 (Figure 5D, E).

Serine protease entry across the intestinal mucin layer

Next, we investigated whether increased levels of enzymatic activity in the intestinal wall were coupled with disruption of mucin. Superposition of protease activity with mucin2 immunofluorescence revealed no detectable co-localization of protease activity and mucin within the accuracy of the experiment (image resolution, and digital analysis) (Figure 6A). In the ischemic experimental groups as mucin2 was disrupted from the villus tips, proteases were observed to penetrate the villi (Figure 6B, C). Furthermore, we detected increased enzymatic activity in the submucosa at 30 min ischemia and enhanced protease activity at the level of the crypts co-localized in the area of the Paneth cells (Figure 6A–C). Enteral protease inhibition with TA reduced enzyme activity levels to those observed in sham controls but did not restore mucin2 density.

Proteolytic cleavage of the extracellular domain of E-cadherin in rat intestine

Ischemia and reperfusion injury is characterized by disruption of intercellular junctions in epithelium (19). We labeled the intracellular and extracellular domains of E-cadherin to determine whether the epithelial junctions are proteolytically disrupted during ischemia and whether this process can be prevented by enteral TA protease inhibition in our model. In the sham control group both domains of E-cadherin are visible along the entire epithelium of each villus. In contrast, in ischemia visible morphological damage was accompanied by disruption of both domains of E-cadherin. TA treatment preserved intra- and extracellular domains of E-cadherin (Figure 7A, B), an observation that was confirmed by Western blot analysis (Figure 7C, D).

Trypsin enzymatic activity in rat plasma

To determine whether digestive enzymes from the lumen of the intestine are transported into the systemic circulation during ischemia we carried out a gelatin zymography analysis of plasma samples. A band was observed at about 20 kDa, approximately at the same location as the trypsin standard (Figure 8A). The relative density of this band increased in the ischemic group but not in the TA treatment group. Incubation of the gel with 300 mM TA resulted in disappearance of these bands (Figure 8B). Western blot analysis showed elevated protein levels of trypsin and chymotrypsin in plasma of the 30min ischemic groups as compared to plasma of sham controls and plasma of those treated with TA (Figures 8C, 8D).

DISCUSSION

The current results indicate that during splanchnic ischemia there is notable morphological damage to the intestine as early as 15 min and major damage after 30 min which is accompanied by disruption of the mucosal barrier (mucin and epithelial mucosal layers). Damage to the mucosal barrier is observed simultaneously with increased enzymatic activity

NIH-PA Author Manuscript

NIH-PA Author Manuscript

NIH-PA Author Manuscript

of digestive serine proteases (trypsin, chymotrypsin, and elastase) in the wall of the intestine and is followed by increased appearance of trypsin and chymotrypsin protein in plasma.

In this study we show that application of tranexamic acid in the lumen of the intestine significantly prevents intestinal injury. TA is clinically used as an anti-fibrinolytic agent (22, 32), chiefly by inhibition of plasminogen activation. However in higher concentrations TA inhibits trypsin (23), and enterokinase-mediated conversion of trypsinogen to trypsin (22). The clinically recommended oral dose of TA is 1–1.5g (2–3 times daily) (33), which is below the inhibitory range of trypsin activity. In the in-vivo experiments we used TA at a concentration of ~200 mM in the lumen of the intestine, which inhibits trypsin activity by about 80% and is less than the $LD50_{oral}$ in the rat (22).

We determined from in-vivo studies that trypsin and chymotrypsin activities are higher in whole intestine homogenates (tissue + luminal contents) of ischemic groups. In addition, by use of equimolar concentrations of substrates with the same fluorescent hydrolysis product, we determined that during ischemia trypsin exhibits the greatest proteolytic activity as compared to chymotrypsin and elastase. This may explain TA's efficacy in attenuation of intestinal injury in ischemia after enteral administration. In-situ zymography of intestinal tissues demonstrates increased activity of all three enzymes across the intestinal wall of ischemic groups without TA treatment. Furthermore, Western blot analysis confirms increased trypsin and chymotrypsin protein levels in the wall of the ischemic intestine. Our data suggest that enteral treatment with TA prior to ischemia inhibits luminal trypsin activity and consequent pancreatic enzyme activity resulting in decreased proteolysis in the intestinal wall. Based on these results we propose that during ischemia activation of additional luminal trypsin results in subsequent activation of other pancreatic enzymes enabling these enzymes to enter the intestinal wall. Once in the mucosal wall these enzymes may be able to induce activation of MMP-9 and accumulation of neutrophils, as previously reported by Rosario et al (34), resulting in possible further inflammatory sequelae.

Our results indicate that digestive enzymes may be able to enter the intestinal wall as a result of mucin disruption. We show that luminal treatment with TA prior to ischemia prevented disruption of mucin13 (membrane bound mucin) and the carbohydrate portion of mucin but not mucin2 (goblet cell derived mucin), suggesting that mucin2 disruption during ischemia may be via a trypsin-independent mechanism. This idea is supported by low levels of co-labeling between mucin2 and proteases. In the non-ischemic control state, intact mucin is located in both goblet cells and in a layer on the epithelium with low or no enzymatic activity in the intestinal wall. In contrast, enzymatic activity is observed at the tip of the villi in as early as 15 min of ischemia, accompanied by a subsequent decrease in epithelial mucin density. After 30 min of ischemia enhanced enzymatic activity is observed throughout the intestinal wall with near absent mucin labeling on the luminal surface. The lack of co-localization between enzymatic activity and mucin suggests that digestive enzymes are not present in areas with an intact mucin layer, suggesting that the enhanced enzymatic activity observed in the epithelial layer may be due to entry of the digestive enzymes across a compromised mucin layer.

Homotypic interactions of the extracellular domains of E-cadherin are responsible for preserving epithelial cell-cell integrity and may be important in preventing intestinal permeability present in shock (35). In this study we observed loss of both the intra and extracellular domains of E-cadherin during ischemia which was prevented by TA treatment. Disruption of E-cadherin in intestinal ischemia may result in increases in intestinal permeability, thus providing an additional route of entry for digestive enzymes through the intestinal wall.

NIH-PA Author Manuscript

NIH-PA Author Manuscript

NIH-PA Author Manuscript

Finally, gelatin zymography of plasma during intestinal ischemia demonstrates increased enzymatic activity of an enzyme of the same molecular weight as trypsin; although elastase is in the same molecular weight range, it does not cleave gelatin. Western blot demonstrates increased levels of trypsin protein in plasma during ischemia as compared to sham controls, suggesting that the enhanced proteolytic activity of this enzyme may be in part due to trypsin. Further studies to confirm the identity of this enzyme are necessary. The presence of enhanced enzyme activity in plasma during ischemia may in part derive from pancreatic enzymes such as trypsin derived from the ischemic and injured intestine.

Evidence presented in this study indicates that the development of tissue injury observed during early periods of intestinal ischemia is the result of two interconnected processes involving disruption of the mucosal barrier and trypsin activation; although involvement of other proteases from inflammatory cells cannot be ruled out. Disruption of the mucin layer during ischemia allows activated trypsin to make its way across the epithelium where it may activate other enzymes (28) and by proteolytic destruction of epithelial junction proteins open a route of entry for other digestive enzymes to enter the intestinal wall and the systemic circulation resulting in autodigestion.

Acknowledgments

Funding: NIH Grants HL76180 and GM85072 and the UC San Diego Interfaces Graduate Training Program in Interdisciplinary Specialization in Multiscale Biology.

The authors thank Dr. Rafi Mazor, Mr. Tom Alsaigh for their critical review of the manuscript and Dr. Alexander Penn, Dr. Edward Tran, and Mr. Frank Delano for their technical support. This research was supported by NIH Grants HL76180 and GM85072.

Abbreviations

BW	Body Weight
SAO	splanchnic arterial occlusion
TA	tranexamic acid
NS	normal saline

References

1. Perry JF, Smith GA, Yonehiro EG. Intestinal obstruction caused by adhesions; a review of 388 cases. Annals of surgery. 1955; 142(5):810–816. [PubMed: 13269031]
2. Oldenburg WA, Lau LL, Rodenberg TJ, Edmonds HJ, Burger CD. Acute mesenteric ischemia: a clinical review. Arch Intern Med. 2004; 164(10):1054–1062. [PubMed: 15159262]
3. Garofalo M, Borioni R, Nardi P, Turani F, Bertoldo F, Forlani S, Pellegrino A, Chiariello L. Early diagnosis of acute mesenteric ischemia after cardiopulmonary bypass. J Cardiovasc Surg. 2002; 43(4):455–459. [PubMed: 12124551]
4. Cheadle WG, Garr EE, Richardson JD. The importance of early diagnosis of small bowel obstruction. Am Surg. 1988; 54(9):565–569. [PubMed: 3415100]
5. World Health Organization. World Health Statistics Annual. Vol. 2008. 2008.
6. Jones H, Trueman E. National Safety Council: Accident Facts. Journal of Experimental Biology. 1996; 52(1):201–216.
7. Holcomb J, Caruso J, McMullin N, Wade CE, Pearse L, Oetjen-Gerdes L, Champion HR, Lawnick M, Farr W, Rodriguez S, Butler F. Causes of death in US Special Operations Forces in the global war on terrorism: 2001–2004. US Army Med Dep J. Jan-Mar 24–37.2007

NIH-PA Author Manuscript

NIH-PA Author Manuscript

NIH-PA Author Manuscript

8. Deitch EA, Xu DZ, Franko L, Ayala A, Chaudry IH. Evidence Favoring the Role of the Gut as a Cytokine-Generating Organ in Rats Subjected to Hemorrhagic-Shock. Shock. 1994; 1(2):141–146. [PubMed: 7749933]
9. Tamion F, Richard V, Lyoumi S, Daveau M, Bonmarchand G, Leroy J, Thuillez C, Lebreton JP. Gut ischemia and mesenteric synthesis of inflammatory cytokines after hemorrhagic or endotoxic shock. Am J Physiol-Gastr L. 1997; 36(2):G314–G321.
10. Wattanasirichaigoon S, Menconi M, Delude R, Fink M. Effect of mesenteric ischemia and reperfusion or hemorrhagic shock on intestinal mucosal permeability and ATP content in rats. Shock. 1999; 12(2):127. [PubMed: 10446893]
11. Sutherland NG, Bounous G, Gurd FN. Role of intestinal mucosal enzymes in the pathogenesis of shock. J Trauma. 1968; 8(3):350–380. [PubMed: 5655160]
12. Mitsuoka H, Kistler EB, Schmid-Schönbein GW. Generation of in vivo activating factors in the ischemic intestine by pancreatic enzymes. Proc Natl Acad Sci U S A. 2000; 97(4):1772–1777. [PubMed: 10677533]
13. Waldo SW, Rosario HS, Penn AH, Schmid-Schönbein GW. Pancreatic digestive enzymes are potent generators of mediators for leukocyte activation and mortality. Shock. 2003; 20(2):138–143. [PubMed: 12865657]
14. Deitch E, Shi H, Lu Q, Feketeova E, Xu D. Serine proteases are involved in the pathogenesis of trauma-hemorrhagic shock-induced gut and lung injury. Shock. 2003; 19(5):452. [PubMed: 12744489]
15. Mitsuoka H, Schmid-Schönbein GW. Mechanisms for blockade of in vivo activator production in the ischemic intestine and multi-organ failure. Shock. 2000; 14(5):522–527. [PubMed: 11092684]
16. Fitzal F, DeLano F, Young C, Rosario H, Schmid-Schönbein G. Pancreatic protease inhibition during shock attenuates cell activation and peripheral inflammation. Journal of vascular research. 2000; 39(4):320–329. [PubMed: 12187122]
17. Penn A, Schmid-Schönbein G. The intestine as source of cytotoxic mediators in shock: free fatty acids and degradation of lipid-binding proteins. American Journal of Physiology- Heart and Circulatory Physiology. 2008; 294(4):H1779. [PubMed: 18263716]
18. Bansil R, Stanley E, LaMont JT. Mucin biophysics. Annu Rev Physiol. 1995; 57:635–657. [PubMed: 7778881]
19. Bush KT, Tsukamoto T, Nigam SK. Selective degradation of E-cadherin and dissolution of E-cadherin-catenin complexes in epithelial ischemia. Am J Physiol Renal Physiol. 2000; 278(5):F847–852. [PubMed: 10807598]
20. Rupani B, Caputo FJ, Watkins AC, Vega D, Magnotti LJ, Lu Q, Xu da Z, Deitch EA. Relationship between disruption of the unstirred mucus layer and intestinal restitution in loss of gut barrier function after trauma hemorrhagic shock. Surgery. 2007; 141(4):481–489. [PubMed: 17383525]
21. Haglund U, Abe T, Ahren C, Braide I, Lundgren O. The intestinal mucosal lesions in shock. I. Studies on the pathogenesis. Eur Surg Res. 1976; 8(5):435–447. [PubMed: 1086771]
22. Andersson L, Nilsson IM, Niléhn JE, Hedner U, Granstrand B, Melander B. Experimental and Clinical Studies on AMCA, the Antifibrinolytically Active Isomer of p Aminomethyl Cyclohexane Carboxylic Acid. Scandinavian Journal of Haematology. 1965; 2(3):230–247. [PubMed: 5834403]
23. Dubber AHC, McNicol G, Douglas A. Amino methyl cyclohexane carboxylic acid (AMCHA), a new synthetic fibrinolytic inhibitor. British Journal of Haematology. 1965; 11(2):237–245. [PubMed: 14262183]
24. Harlow, E.; Lane, D. Antibodies: a laboratory manual. CSHL press; 1988.
25. Zimmerman M, Ashe B, Yurewicz EC, Patel G. Sensitive assays for trypsin, elastase, and chymotrypsin using new fluorogenic substrates. Anal Biochem. 1977; 78(1):47–51. [PubMed: 848756]
26. Castillo MJ, Nakajima K, Zimmerman M, Powers JC. Sensitive substrates for human leukocyte and porcine pancreatic elastase: a study of the merits of various chromophoric and fluorogenic leaving groups in assays for serine proteases. Anal Biochem. 1979; 99(1):53–64. [PubMed: 394626]
27. Zimmerman M, Yurewicz E, Patel G. A new fluorogenic substrate for chymotrypsin. Anal Biochem. 1976; 70(1):258–262. [PubMed: 1259147]

NIH-PA Author Manuscript

NIH-PA Author Manuscript

NIH-PA Author Manuscript

28. Rosario HS, Waldo SW, Becker SA, Schmid-Schönbein GW. Pancreatic trypsin increases matrix metalloproteinase-9 accumulation and activation during acute intestinal ischemia-reperfusion in the rat. Am J Pathol. 2004; 164(5):1707–1716. [PubMed: 15111317]

29. Yi CF, Gosiewska A, Burtis D, Geesin J. Incorporation of fluorescent enzyme substrates in agarose gel for in situ zymography. Anal Biochem. 2001; 291(1):27–33. [PubMed: 11262153]

30. Gawlak M, Gorkiewicz T, Gorlewicz A, Konopacki FA, Kaczmarek L, Wilczynski GM. High resolution in situ zymography reveals matrix metalloproteinase activity at glutamatergic synapses. Neuroscience. 2009; 158(1):167–176. [PubMed: 18588950]

31. Hibbs M, Hasty K, Seyer J, Kang A, Mainardi C. Biochemical and immunological characterization of the secreted forms of human neutrophil gelatinase. Journal of Biological Chemistry. 1985; 260(4):2493. [PubMed: 2982822]

32. Nilsson IM. Clinical pharmacology of aminocaproic and tranexamic acids. Journal of Clinical Pathology. 1980; 33(Suppl 14):41. [PubMed: 7000846]

33. Dunn CJ, Goa KL. Tranexamic acid: a review of its use in surgery and other indications. Drugs. 1999; 57(6):1005–1032. [PubMed: 10400410]

34. Fitzal F, DeLano F, Young C, Rosario H, Junger W, Schmid-Schönbein G. Pancreatic enzymes sustain systemic inflammation after an initial endotoxin challenge. Surgery. 2003; 134(3):446–456. [PubMed: 14555932]

35. Doig CJ, Sutherland LR, Sandham JD, Fick GH, Verhoef M, Meddings JB. Increased intestinal permeability is associated with the development of multiple organ dysfunction syndrome in critically ill ICU patients. Am J Respir Crit Care Med. 1998; 158(2):444–451. [PubMed: 9700119]

NIH-PA Author Manuscript

NIH-PA Author Manuscript

NIH-PA Author Manuscript

A

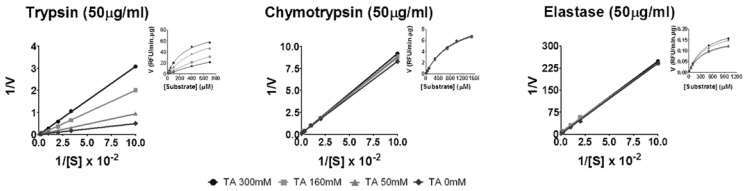

B

[TA]	Trypsin			Chymotrypsin			Elastase		
	V_{max}	K_m	R^2	V_{max}	K_m	R^2	V_{max}	K_m	R^2
300mM	81± 9	1915± 267	0.998	11± 0.4	972± 61	0.998	0.17± 0.004	364± 21	0.998
160mM	97± 8	1451± 163	0.998	11± 0.3	999± 44	0.999	0.16± 0.004	389± 26	0.997
50mM	87± 3	579± 41	0.998	11± 0.4	985± 73	0.997	0.21± 0.007	425± 37	0.996
0mM	84± 3	306± 22	0.996	11± 0.3	911± 51	0.998	0.23± 0.006	424± 26	0.998

Figure 1.

Lineweaver-Burk Plot with inset Michaelis-Menten plot showing Inhibitory profile of Tranexamic Acid in-vitro as determined by titration against added trypsin, chymotrypsin and elastase using fluorescent substrates specific for these enzymes. Values are mean±SEM of triplicate measurements, symbols used: TA 300mM (circle), TA 160mM (square), TA 50mM (triangle), TA 0mM (diamond) (**A**). Enzyme kinetic parameters, V_{max} (RFU/min.μg), K_m (μM) for the enzymes with different concentrations of TA calculated after non-linear regretion **(B)**

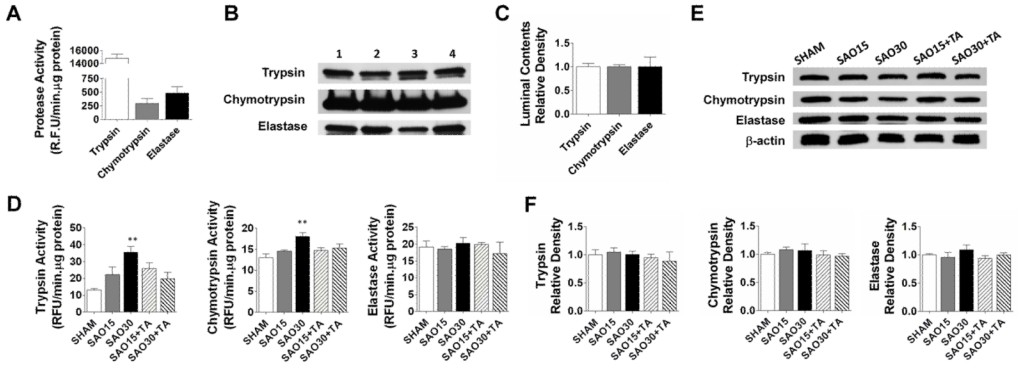

Figure 2.

Activity of trypsin, chymotrypsin and elastase in intestinal luminal contents of sham animals using substrates specific for these enzymes (A). Western blot of intestinal luminal contents for the enzymes; values are mean±SEM (n=4) **(B, C)**. In-vivo enzymatic activity of trypsin, chymotrypsin and elastase in whole intestine homogenates without removal of luminal contents **(D)**. Western blot of whole intestine homogenates for the three enzymes; values are mean±SEM (n=4)/group ** P<0.001 compared to sham **(E, F)**.

NIH-PA Author Manuscript NIH-PA Author Manuscript NIH-PA Author Manuscript

NIH-PA Author Manuscript

NIH-PA Author Manuscript

NIH-PA Author Manuscript

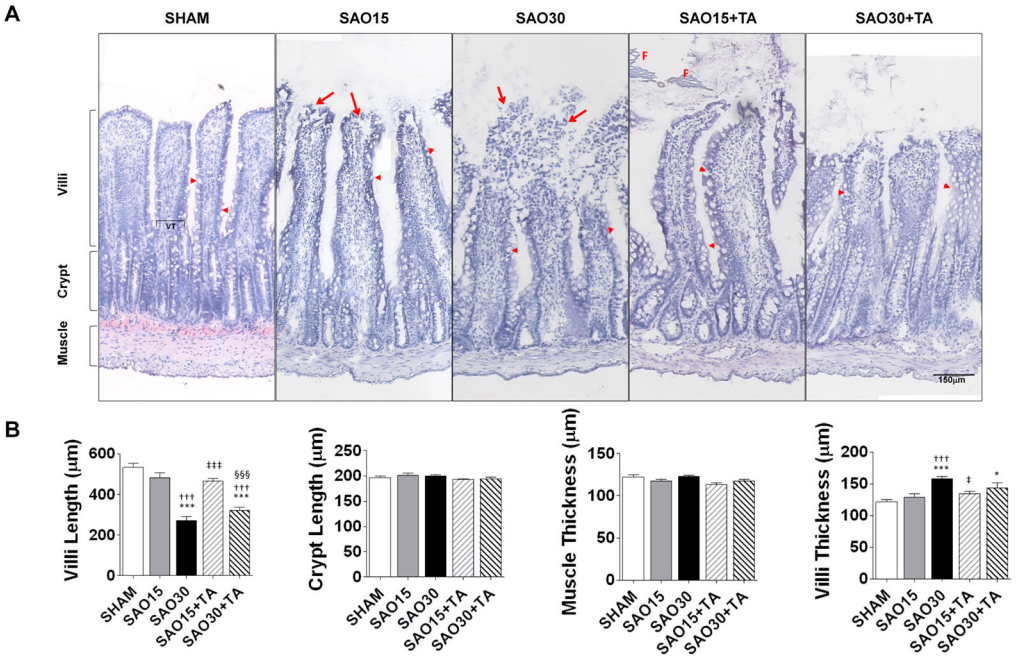

Figure 3.

Representative Micrographs of jejunal frozen sections stained with hematoxylin and eosin (**A**). The sections were derived from frozen segments without removal of luminal food (F) or other luminal contents. Arrowheads show goblet cells and arrows show degeneration of villi. Mean length of villi and crypts as well as mean muscle layer and villi thickness (VT) (**B**). Values are mean±SEM (n=4)/group. *P <0.05, ***P<0.0001 compared to sham. †††P<0.0001 compared to 15 min SAO. ‡‡‡P<0.0001 compared to 30 min SAO, §§§P<0.0001 compared to 15 min SAO with Tranexamic Acid.

NIH-PA Author Manuscript
NIH-PA Author Manuscript
NIH-PA Author Manuscript

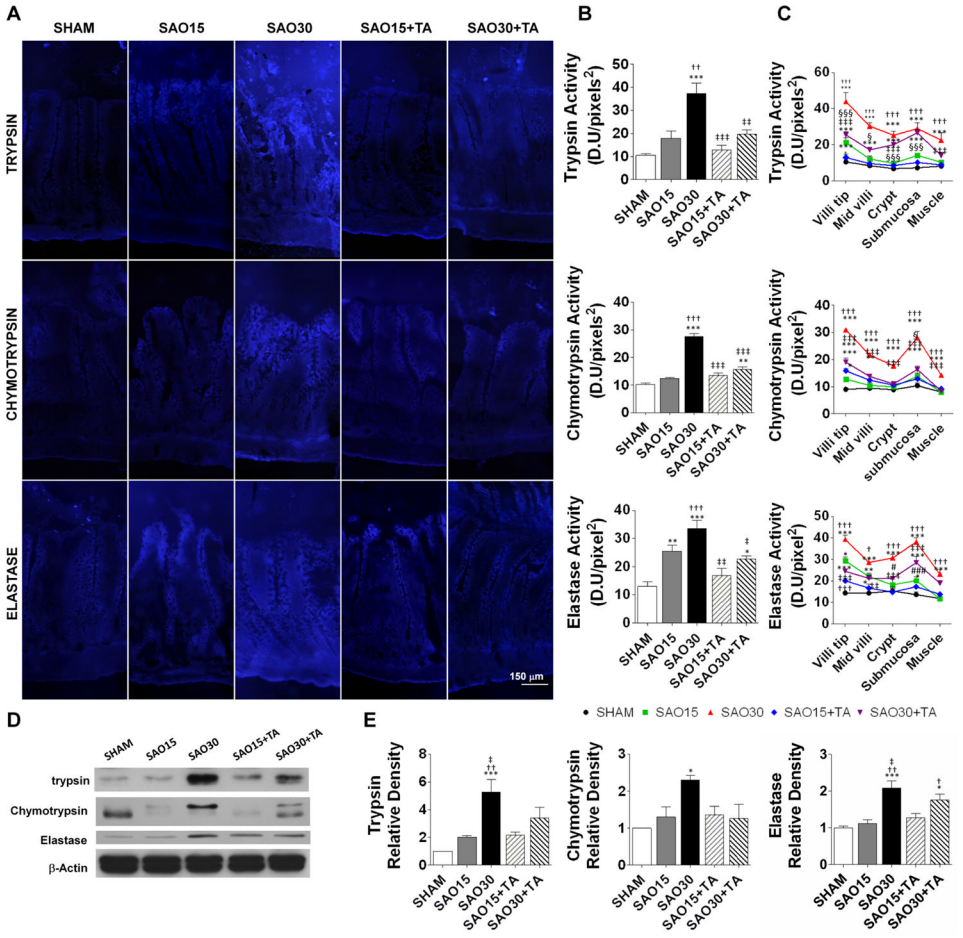

Figure 4.

Representative micrograph of enzymatic activity on jejunal sections (4/animal) as assessed by *in-situ* zymography of substrates specific for trypsin, chymotrypsin and elastase (**A**). Enzymatic activity measured on the micrographs as mean fluorescent intensity of the fluorescent substrates, values are mean±SEM (n=4)/group (**B**). Enzyme penetration from the villi tip to the intestinal muscle measured on the micrographs (4/animal) as mean fluorescent intensity of the fluorescent substrates. Values are mean±SEM (n=4)/group, symbols used: Sham (circle), SAO15 (square), SAO30 (triangle) SAO15+TA (diamond), SAO30+TA (inverted triangle) (**C**). Western blot of trypsin, chymotrypsin and β-actin in intestine homogenates after removal of luminal contents (**D**). Relative density of trypsin and chymotrypsin and elastase with respect of β-actin. Values are mean±SEM (n=4)/group (**E**). *P <0.05, **P<0.001, ***P<0.0001 compared to sham. †P <0.05, ††P<0.001, †††P<0.0001 compared to 15 min SAO. ‡P <0.05, ‡‡P<0.001, ‡‡‡P<0.0001 compared to 30 min SAO.

NIH-PA Author Manuscript

NIH-PA Author Manuscript

NIH-PA Author Manuscript

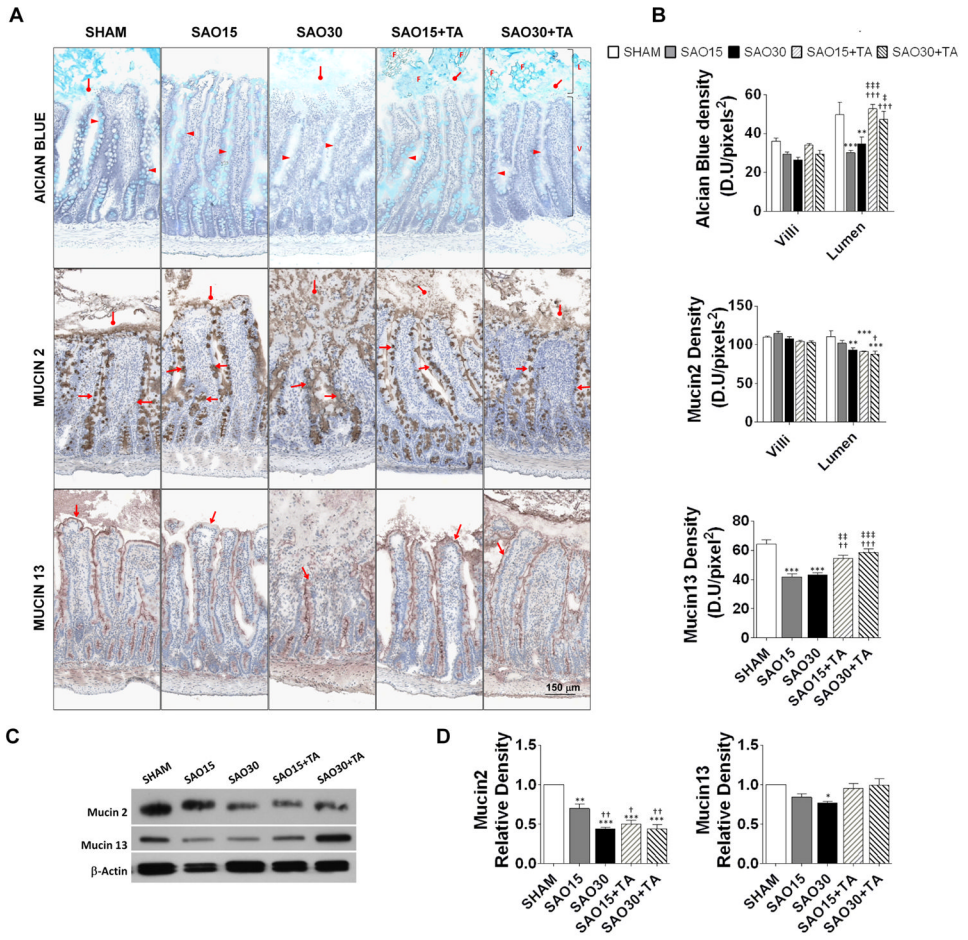

Figure 5.

Representative micrographs of jejunal frozen sections stained with alcian blue specific for the carbohydrate domain of mucin and immunoperoxidase staining against goblet cell-derived mucin2 and membrane-bound mucin13 (4/animal) (**A**). The intestinal lumen (L), villi (V) and luminal food (F) residues are visible; arrowheads show mucin in goblet cells, diamond arrows demonstrate luminal mucin and arrows show membrane-bound mucin. Mucin density measured as the mean light intensity after labeling with alcian blue or primary antibody against mucin2 or mucin13 with DAB substrate. Values are mean±SEM (n=4)/group, color symbols used: Sham (white), SAO15 (gray), SAO30 (black), SAO15+TA (gray diagonal lines), SAO30+TA (black diagonal lines) (**B**). Western blot of mucin2, mucin13 and β-actin in intestine homogenates with removal of luminal contents (**C**). Relative density of mucin2 and mucin13 with respect of β-actin (**D**). Values are mean±SEM (n=4)/group. *P <0.05, **P<0.001, ***P<0.0001 compared to sham. †P<0.05, ††P<0.001, †††P<0.0001 compared to 15 min SAO. ‡P<0.05, ‡‡P<0.001, ‡‡‡P<0.0001 compared to 30 min SAO.

NIH-PA Author Manuscript

NIH-PA Author Manuscript

NIH-PA Author Manuscript

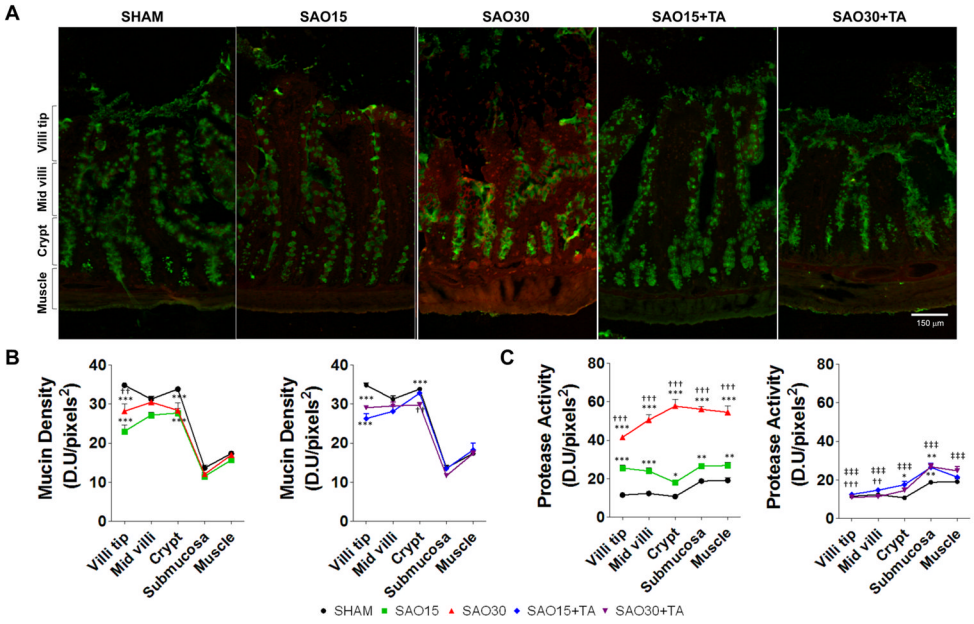

Figure 6.

Representative micrographs of jejunal frozen sections with immunofluorescent labeling against mucin2 (green) and *in-situ* zymography of casein substrate specific for serine proteases (red) (**A**). Mucin density in different regions of the villi as measured by the mean light intensity of FITC; data presented in two graphs: Sham and SAO and sham and SAO +TA treatment (**B**). Serine protease activity in different regions of the villi as measured by the mean light intensity of the Texas Red label; data presented in two graphs: Sham and SAO and sham and SAO+TA treatment (**C**). Values are mean±SEM (n=4)/group. Symbols used: SHAM (circle), SAO15 (square), SAO30 (triangle), SAO15+TA (diamond), SAO30+TA (inverted triangle).*P <0.05, **P<0.001, ***P<0.0001 compared to sham. ††P<0.001, ††P<0.001, †††P<0.0001 compared to 15 min SAO. ‡‡‡P<0.0001 compared to 30 min SAO, ##P<0.001, §§§P<0.0001 compared to 15 min SAO with TA. Figures are displayed as sham and SAO and sham and SAO plus TA for better visualization.

NIH-PA Author Manuscript

NIH-PA Author Manuscript

NIH-PA Author Manuscript

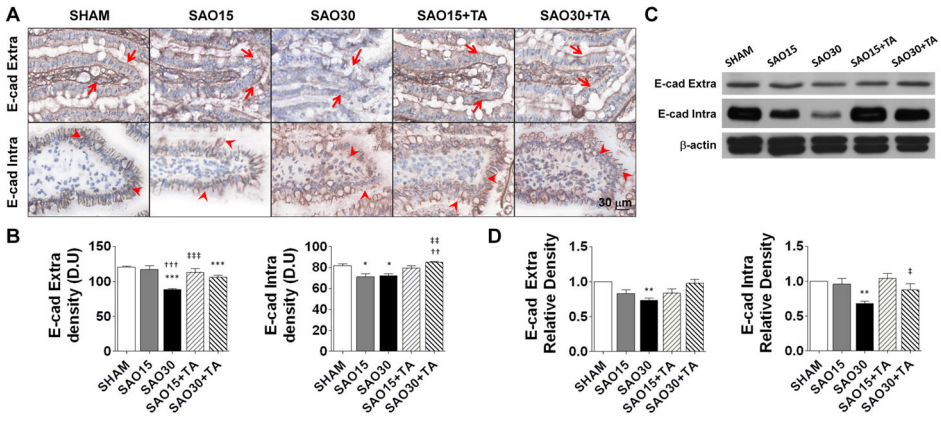

Figure 7.

Representative micrographs of the villus tip from jejunal frozen sections oriented horizontally. Arrows represent immunoperoxidase staining against the extracellular domain of E-caherin and arrowheads represent staining agains intracellular domains of E-cadherin (**A**). E-cadherin density measured as the mean light intensity after labeling with primary antibody against extracellular and intracellular domain of E-cadherin and DAB substrate, values are mean±SEM (n=4)/group (**B**). Western blots of both intra- and extra-cellular domains in intestine homogenates with removal of luminal contents (**C**). Relative density of intra and extra-cellular domains with respect of β-actin. Values are mean±SEM (n=4)/group (**D**). *P <0.05, ***P<0.0001 compared to sham. ††P<0.001, †††P<0.0001 compared to 15 min SAO. ‡‡P<0.001, ‡‡‡P<0.0001 compared to 30 min SAO, §§§P<0.0001 compared to 15 min SAO with TA.

NIH-PA Author Manuscript

NIH-PA Author Manuscript

NIH-PA Author Manuscript

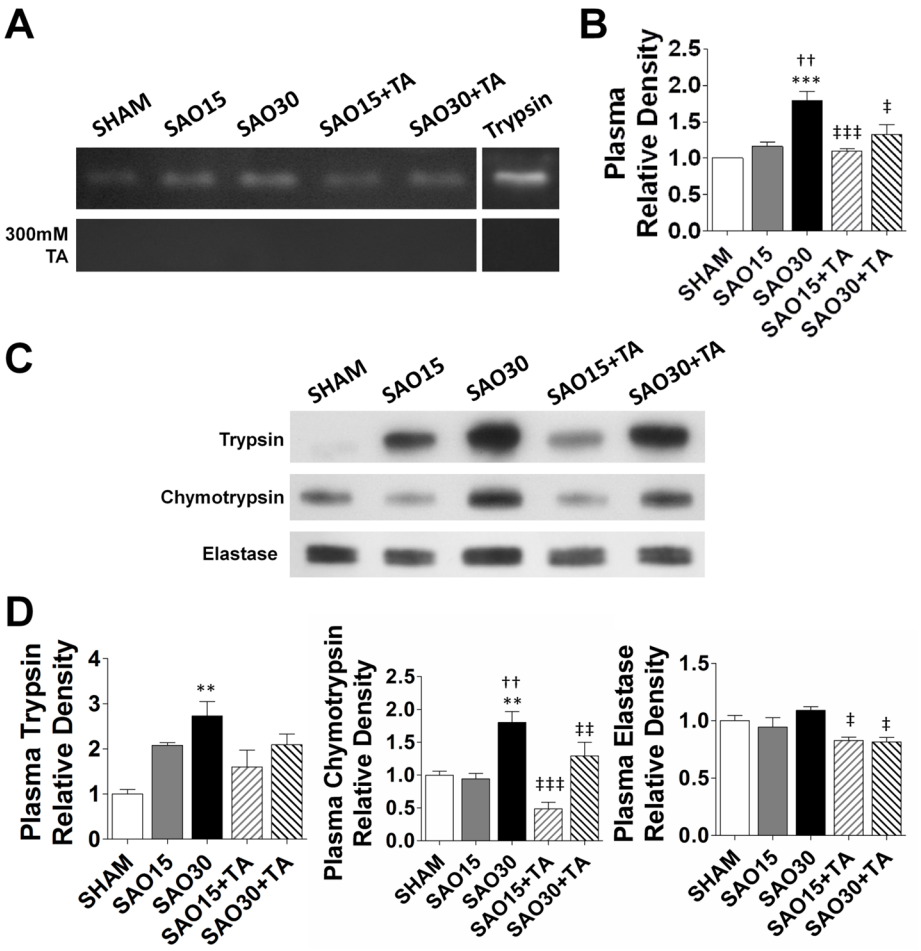

Figure 8.

Gelatin zymography of plasma without and with Tranexamic acid inhibition during renaturing and developing steps. Bands correspond to about 20kDa molecular weight (**A**) Relative density of proteolytic enzyme activity, values are mean±SEM (n=4/group) (**B**). Western blot of trypsin, chymotrypsin, and elastase in plasma (**C**). Relative density of the three enzymes in plasma; values are mean±SEM (n=4/group) (**D**). *P <0.05, ***P<0.0001 compared to sham. ††P<0.001, †††P<0.0001 compared to 15 min SAO. ‡‡P<0.001, ‡‡‡P<0.0001 compared to 30 min SAO, §§§P<0.0001 compared to 15 min SAO with TA.